Integrated Multimode Orbital Angular Momentum Antenna Based on RF Switch

YONG-XING DU, HUAN LIU, LING QIN, AND BAO-SHAN LI
School of Information Engineering, Inner Mongolia University of Science and Technology, Baotou 014010, China

Corresponding author: Ling Qin (qinling1979@imust.edu.cn)

ABSTRACT This paper proposes an electronically reconfigurable multimode orbital angular momentum (OAM) patch array antenna using single pole double throw radio frequency switch that can complete dynamic switching of three modes (−1,0,1) at 2.4 GHz. As a new type of multiplexing technology, the application value of OAM technology in radar imaging and wireless communication has been continuously verified. Considering that many theoretical algorithms are proposed, a multimode vortex antenna that meets the experimental requirements should be developed. The proposed antenna consists of RF switch, programmable microcontroller, phase-shifted feed network, and 2 × 2 rectangular array. Different feeder networks were selected by controlling the RF switch to generate vortex beams with different modes. The proposed antenna was numerically simulated and physically produced. The feasibility of the design was verified through experiments. The simulation and design results are basically the same. The proposed scheme has simple structure, easy to design and deploy, and has important significance in the design of many mode vortex antenna applications in communication and radar imaging.

INDEX TERMS Multimode, orbital angular momentum, reconfigurable, RF switch, vortex antenna.

I. INTRODUCTION

With the increasing application of 5G and Internet of Things (IOT) technologies, wireless communication has experienced many opportunities and challenges in recent years. The demand for wireless spectrum rapidly increases to provide convenience for users, and a new method should be fundamentally developed to upgrade wireless communication technology. Orbital angular momentum (OAM), similar to the four other features, has a great development prospect and good directionality as a new dimension feature of electromagnetic waves, and has great research value in information security. Designing antennas using OAM technology will increase the utilization of communication resources to a great extent.

The study of OAM is derived from the prophecy of Poynting in 1909 [1]. In 1936, Beth detected and measured the angular momentum of polarized light passing through the crystal plate using a special method. In 1981, the

The associate editor coordinating the review of this manuscript and approving it for publication was Chow-Yen-Desmond Sim.

vortex structure was discovered by Baranova in the analysis and exploration of speckle field experiments. In 1989, Coullet *et al.* analyzed the problems in the field of optics and first proposed the concept of ''optical vortex.'' This concept was theoretically defined and elaborated. In 2007, Thide *et al.* first studied OAM in a low-frequency environment using a software method by emitting a wireless signal with Gaussian beam characteristics using a phased array [2]. Their study is the first to apply OAM in wireless communications through related technologies, which is extremely important. In 2008, Carc-Escartion *et al.* conducted an in-depth analysis of optical OAM multiplexing techniques [3]. In 2012, the University of California used an experimental method to realize the application of OAM multiplexing technology in communication in the field of optics. Mahmouli and Walker realized video transmission at 60 GHz through a laboratory experiment [4]. In the same year, Wang. J, *et al.* of Huazhong University of Science and Technology used a stepped reflector antenna based on OAM to complete information transmission in tbps [5], and the spectral efficiency reaches 95.7 bit/s/Hz. In 2013, a French team proposed a method to change

the dielectric constant for achieving different phase feeds. Dr. D. Zelenchuk of the United Kingdom used a rotating phase plate method to complete the generation of 10 GHz vortex waves. In the same year, the Chinese Academy of Sciences developed vortex wave communication as a prere-search project. In 2016, a research team at Tsinghua University successfully designed and completed the first microwave band OAM electromagnetic wave transmission with 27.5 km distance.

The principle of vortex electromagnetic wave is to add a phase factor to the plane electromagnetic wave, thereby enabling the electromagnetic wave radiated into the free space to have a spiral wavefront structure. At present, the methods for designing an antenna capable of generating a vortex electromagnetic wave mainly include an array antenna, a transmission grating [6], [7], a spiral phase plate, and a parabolic antenna. The antenna is divided into a feed antenna and an array antenna depending on the production method [8], and the feed antenna is divided into a reflection type and a transmission type. The reflective type has a spiral parabolic antenna, a porous medium reflection array, and a spiral phase plate. The transmission type has a feed network array antenna and a phased array antenna [9]. The array antenna enables each antenna unit to have different phases by designing different feed networks. The phased array antenna generates OAM electromagnetic waves through the time switch array, thereby causing the feed delay.

As a device for radiating vortex beams, a vortex antenna needs to meet the application requirements of the OAM related characteristics - multiple mode multiplexing transmission. OAM has great application value because of its multiplexed transmission noninterference characteristics. Designing a multimode vortex antenna and continuous switching mode based on the traditional vortex antenna has been widely investigated. At present, the commonly used switching device in practice is a pin diode [10]–[15], which has the same function as a multichannel radio frequency (RF) switch. However, the latter can immensely reduce the number of devices used and conserve controller pin resources in actual design.

This paper proposes an electronic reconfigurable multimode OAM patch array antenna using single pole double throw (SPDT) RF switch that can complete dynamic switching of three modes (−1,0,1) at 2.4 GHz. The RF switch is controlled through the programmable microcontroller (STC89C52RC) to select the different phase-shifted feeder networks for dynamically switching the OAM mode. The feasibility of radiating vortex electromagnetic waves of microstrip array antennas and the scheme of reconfigurable vortex antennas is designed and discussed in [5].

II. VORTEX ELECTROMAGNETIC WAVE PRINCIPLE
The study of OAM originates in the field of optics. It has been vigorously developed in wireless communications in recent years. Two feature quantities are found during wave propagation in free space. Among them, OAM is a
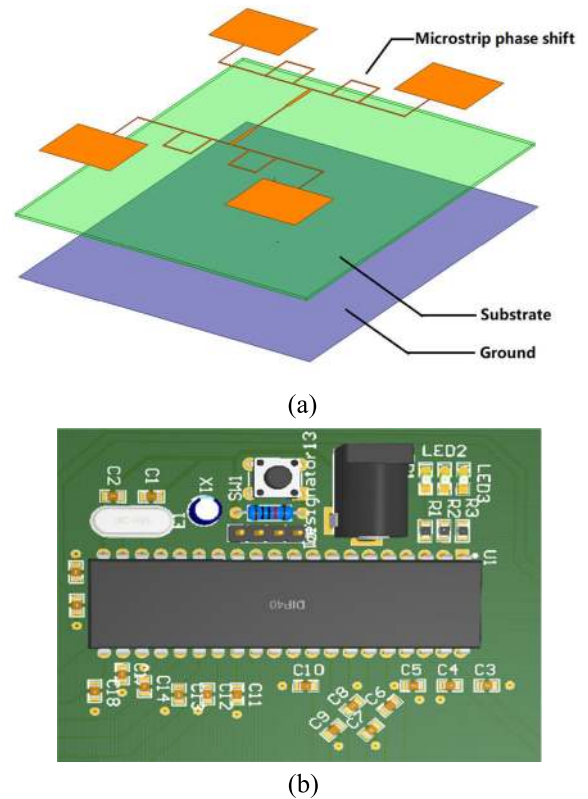

(a)

(b)

FIGURE 1. **Structural decomposition of the multimode OAM antenna system. (a) Antenna part perspective, (b) 3D top view of the control circuit section.**

feature associated with the 3D structure. The OAM and phase wavefronts are different. The angular momentum of the electromagnetic field on the basis of classical dynamics [16], [17] can be expressed as follows:

$$J = \int \varepsilon_r \times \mathrm{Re} \left| E \times B^* \right| dV \qquad (1)$$

$$J = L + S \qquad (2)$$

In particular:

$$\int_0^{2\pi} e^{il_1\varphi} \left(e^{il_2\varphi} \right)^* d\varphi = \begin{cases} 2\pi, & l_1 = l_2 \\ 0, & l_1 \neq l_2 \end{cases} \qquad (3)$$

$$S = \varepsilon \int \mathrm{Re}\left\{ E^* \right\} dV \qquad (4)$$

$$\vec{L} = -\mathrm{i}(r \times \nabla) \qquad (5)$$

where L represents the OAM, and S represents the spin angular momentum. $\vec{L} = -\mathrm{i}(r \times \nabla)$ represents the vector operator of OAM, $\vec{A}$ represents a vector bit function, the theoretical analysis of spin angular momentum has three different modes, and the OAM theoretically has a myriad of different modes. As shown in Equation 2, the OAM is related to the position vector and electromagnetic wavefront. The vortex electromagnetic wave carrying OAM is expressed as:

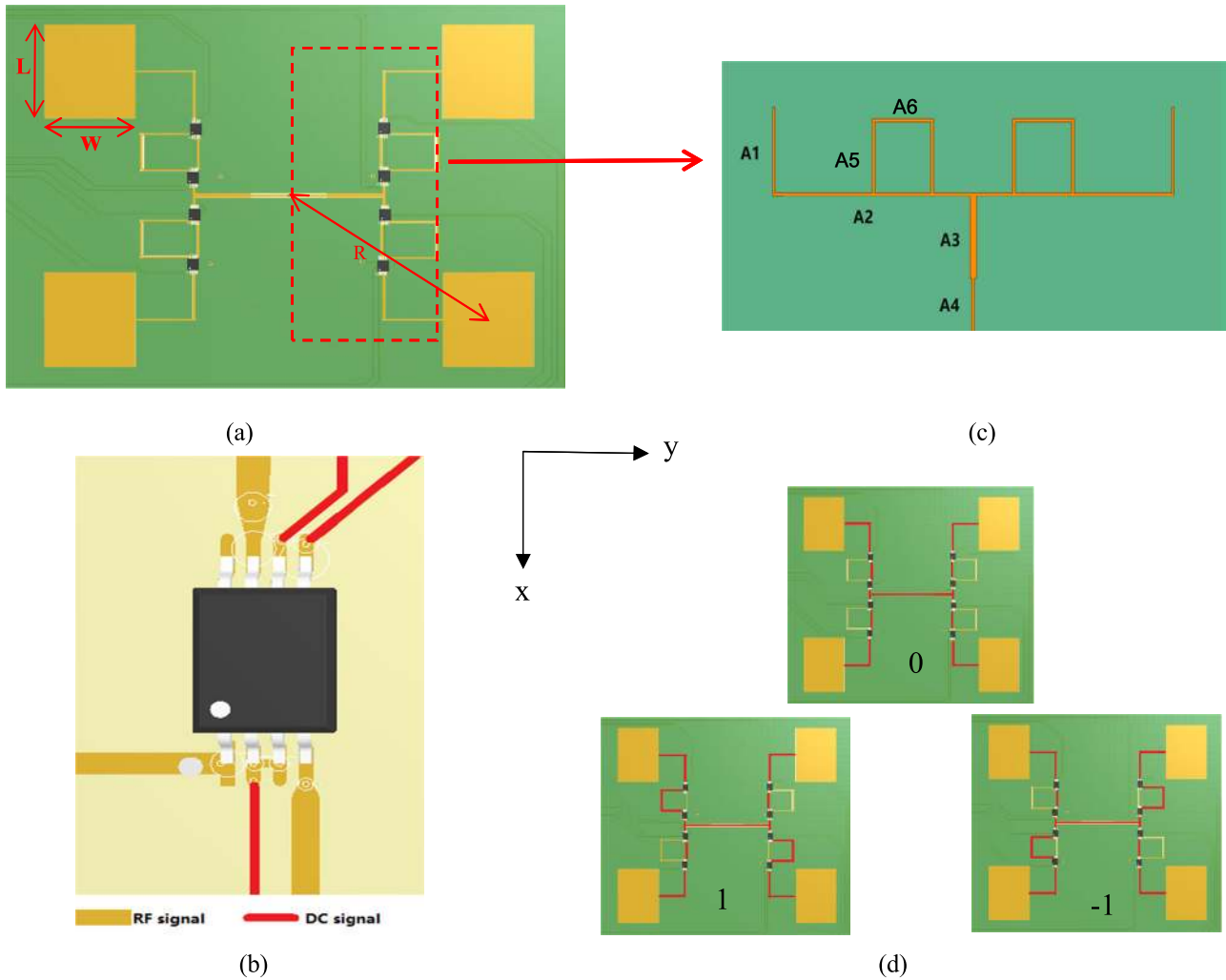$$U(r, \varphi) = A(r) \cdot e^{il\varphi} \qquad (6)$$

(a)

(b)

(c)

(d)

FIGURE 2. Microstrip antenna part schematic. (a) Antenna part perspective, (b) Chip pin connection diagram. (c) Feed network, (d) Schematic of −1,0,1 mode feed network reconstruction.

$A(r)$ represents the amplitude of the signal, r represents the radius of radiation, φ represents the azimuth angle, and l represents the mode of the generated electromagnetic wave.

As shown in the following formulas [18], [19], multiplex transmission of the OAM can be realized without interference because the vortex electromagnetic waves of different modalities are orthogonal to each other, making it suitable in the field of communication.

The empirical formula based on the vortex electromagnetic wave is expressed as:

$$\Delta\varphi = \frac{2\pi l}{N} \tag{7}$$

$$-\frac{N}{2} < l < \frac{N}{2} \tag{8}$$

where N represents the number of array elements of the array antenna, $\Delta\varphi$ represents the phase difference between the array elements, and l represents the number of modes.

The designed antenna in this solution uses the principle of a switched-line phase shifter and the switching delay line

technology of SPDT switch to control microwave signals for passing through two transmission lines with different electrical lengths to obtain different phase states $\Delta\phi$. The difference between the phase shifts of the two states is determined by electrical length ΔL of the two paths:

$$\Delta\phi = \frac{2\pi}{\lambda} \times \Delta L \tag{9}$$

III. ANTENNA SYSTEM SOLUTION

The proposed multimode OAM antenna structure is shown in Fig. 1. The entire antenna system is divided into two parts, namely, the microstrip antenna and the control circuit. As shown in Figure 1 (a), the microstrip antenna has a three-layer structure, namely, a radiant piece, a dielectric substrate, and a ground plane from top to bottom. The phase shifting part of the feed network is added, and the working principle is described in detail later. Fig. 1 (b) shows the 3D top view of the control circuit section. Sixteen channels of DC signals are generated to drive the RF switch.
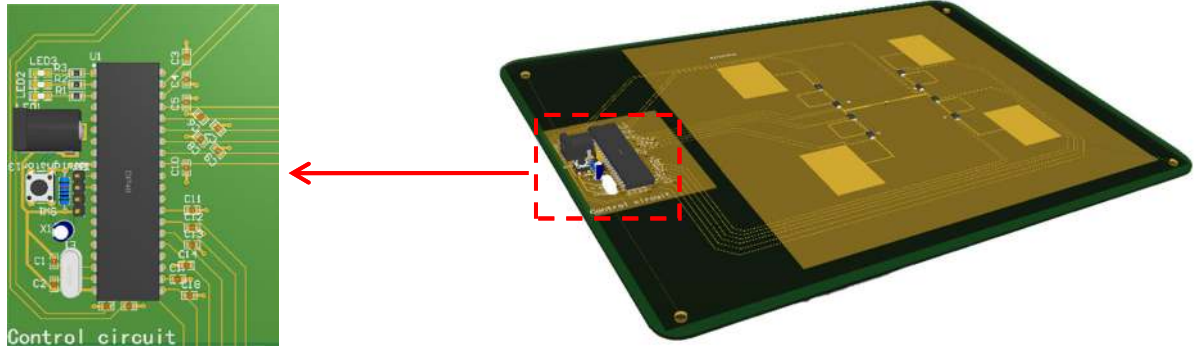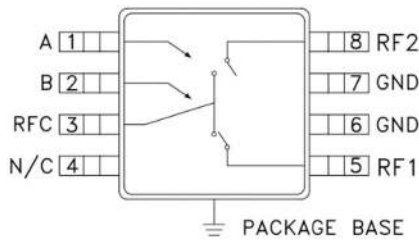
FIGURE 3. Schematic of control circuit.

FIGURE 4. Switch chip pin description.

TABLE 1. Truth table.

Control input		Signal path state
A	B	RFC to:
Low	High	RF1
High	Low	RF2

FIGURE 5. Chip numbering diagram.

TABLE 2. Different modes of pin status.

Chip Number	0 A	0 B	1 A	1 B	−1 A	−1 B
1	High	Low	Low	High	High	Low
2	Low	High	High	Low	Low	High
3	High	Low	High	Low	Low	High
4	Low	High	Low	High	High	Low
5	Low	High	Low	High	High	Low
6	High	Low	High	Low	Low	High
7	Low	High	High	Low	Low	High
8	High	Low	Low	High	High	Low

TABLE 3. Designed parameter values of the OAM antenna (Size: mm).

NO.	Parameters	Value, mm
1	L	37.2
2	W	27.95
3	R	78.4
4	A1	0.47
5	A2	0.68
6	A3	1.59
7	A4	11.7
8	A5	15.3
9	A6	15

consisting of two RF switches and phase shifting microstrip lines. Figure 2 (c) shows the feed network. The length and width of A1–A4 segments are designed on the basis of the microstrip line impedance matching principle. The reconstruction of different mode switching feed network is shown in Figure 2 (d). Different signal paths are selected by controlling the RF switch, thereby enabling the signal arriving at the radiating patch to have a certain phase difference. Figure 2 (b) shows the connection diagram of the switch chip, where the DC signal is represented in red, and the RF signal is represented in yellow. The microstrip line connected to the RF pin is subjected to tearing treatment to minimize the loss in the RF signal transmission. The RF signal input adopts the coaxial feeding mode. The diameter of the grounding area of the mounting hole is larger than the diameter of the dielectric
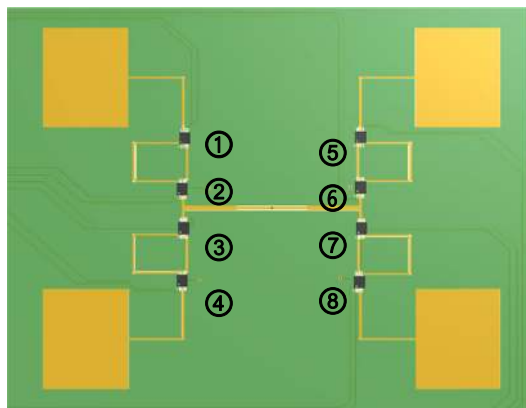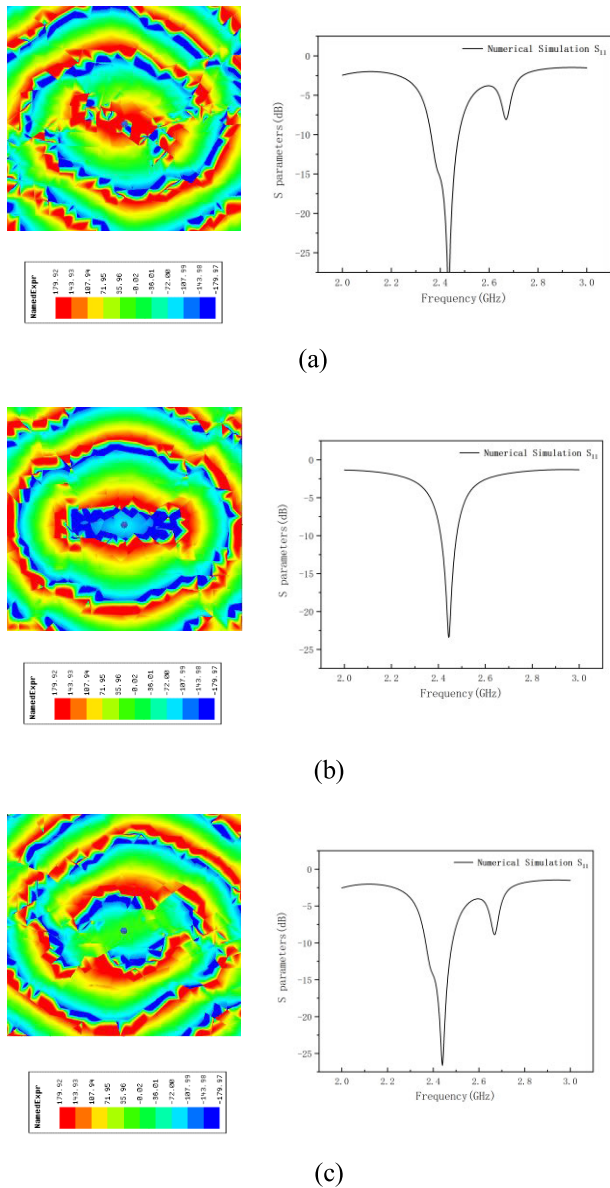
A. RADIATION PATCH AND FEED NETWORK DESIGN

As shown in Figure 2 (a), the antenna portion consists of a four-element microstrip patch array and a reconfigurable phase-shifted feed network.

Four phases shifting units are found, and each phase shifting unit can provide 0° or 90° signal phase shift,

(a)

(b)

(c)

FIGURE 6. Simulated electric field phase (upper) and S11 (lower) distribution at 2.4 GHz for (a) *l* = +1, (b) *l* = 0, (c) *l* = −1.

through hole to prevent signal short circuit because the signal axis of the SMA head cannot be in contact with the ground plate.

B. CONTROL CIRCUIT SCHEME PRINCIPLE
As shown in Figure 3, the control circuit uses an STC89C52RC microcontroller as the main controller, and the minimum working system is designed on the basis of circuit principle theory. Sixteen DC signals are generated to drive the RF switch chip. The RF chip used is HMC536MS8G. HMC536MS8G is ideal for:

- Cellular/PCS/3G infrastructure
- ISM/MMDS/WiMAX
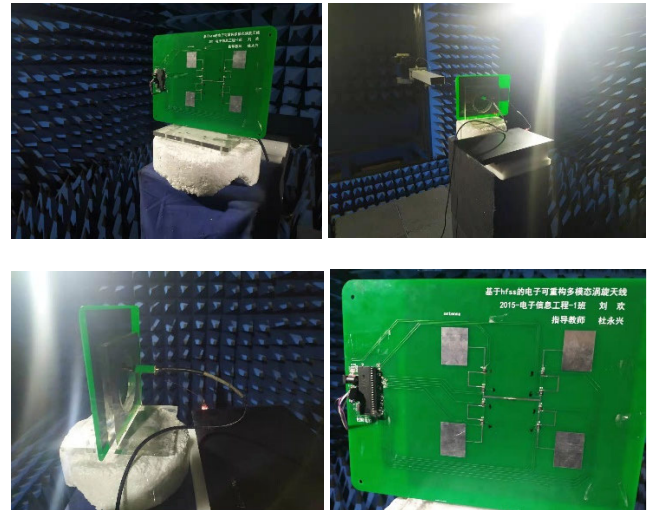- CATV/CMTS
- Test instrumentation

FIGURE 7. Actual processed antenna and test installation diagram.

The RF switch chip has a total of eight pins, three for RF input and output, two for ground, one for floating or ground, and two control pins. After completing the basic control design, a bypass capacitor is introduced on each control line to bypass the high-frequency signal that is returned to the microcontroller and prevent crosstalk between AC and DC. Figure 4 and Table 1 show the operation of the RF switch chip.

The microcontroller used in this design needs approximately 1 μs to execute a statement and takes 10 μs to complete each modal configuration. Theoretically, the proposed antenna can switch to 10^5 times per second.

C. MULTIMODE OAM ANTENNA WORK PRINCIPLE
The pin states of the individual chips in different modes are given in accordance with the chip sequence marked in Figure 5. Three modes can be generated through the combination of different states of the eight switches. The reconstructed feed network is shown in Figure 2 (d).

IV. NUMERICAL SIMULATION AND ACTUAL MEASUREMENT
The numerical simulation analysis of the antenna shown in Fig. 2 (a) was conducted on 3D electromagnetic simulation software HFSS (Ansoft), and the equivalent simulation of the reconstructed antenna under the combination of eight different switch states was performed. The specific microstrip antenna parameters are shown in Table 3. The substrate is FR4, with relative permittivity ε = 4.4, loss tangent tan δ = 0.02, and thickness H = 1.6 mm.

The simulated reflection coefficients of the proposed OAM antenna at different modes are shown in Figure 6 (from top to bottom +1, 0, −1 mode). The designed antennas in different modes are less than −10 dB at 2.4GHz, the frequency of simulated reflection coefficient |S11| < −10 dB ranges from 2.41 GHz to 2.48 GHz for the mode 0, and the
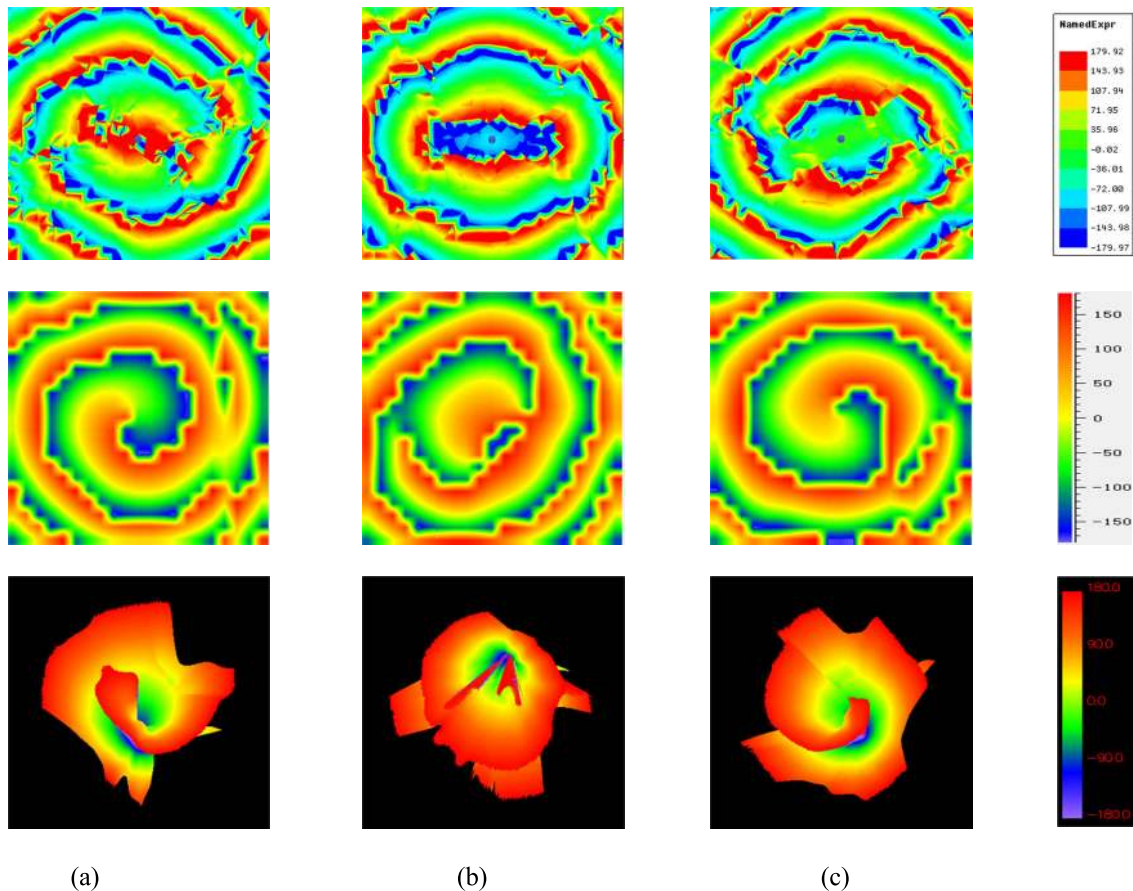
FIGURE 8. Numerical simulation and actual test values of OAM antenna S11 under different modes: (a) +1, (b) 0, (c) −1.

frequency ranges from 2.36 GHz to 2.48 GHz for the mode ±1. As shown in Figures 6 (a) and (c), the phase of the electromagnetic wave radiated by the proposed antenna design at 2.4 GHz has a distinct spiral structure, that is, a vortex electromagnetic wave is generated. The +1 and −1 modes carrying the OAM are smaller than the return loss of 0 mode. The bandwidth is wide, and the frequency selectivity of the three modes is better.

The actual fabricated antenna is shown in Figure 7. The dielectric substrate is FR-4, the chip is hand soldered, and the antenna feed mode is 50 Ω back coaxial feed. The test process controls different combinations of RF switches by programming different programs to generate three modes. Each circuit DC signal voltage in the control circuit is > 4.5 V, and a multimeter is used to verify that the eight chip switches are in normal operation and is sent to the test. The antenna return loss test is conducted using an Agilent vector network analyzer platform. Considering that the antenna control circuit is a DC circuit, the spacer is designed to prevent the DC signal from entering the AC part and causing damage to the LNA and other circuits. Another function of the DC-blocking circuit is to perform secondary impedance matching at the signal feeding. The impedance of the high-frequency signal flowing into or out

of the RF switch is large, thereby seriously affecting the normal operation of the impedance matching network, and the signal loss is extremely large. At the signal feed point, the secondary impedance matching is performed by the DC-blocking circuit. Figure 7 shows the DC matching circuit used in the test.

Experiments were performed in a microwave anechoic chamber to verify the results of simulation analysis [20], [21]. Considering that the electromagnetic waves emitted by the designed antenna have a helical phase wavefront structure, verification of the simulation analysis results requires testing the plane phase distribution in the microwave anechoic chamber to prove the OAM beam. The experimental test chart is shown in Figure 7. The probe uses a rectangular waveguide and is placed in strict alignment with the center of the antenna.

The waveguide is 600 mm from the antenna plane, the detection plane size is 110 mm × 110 mm, and the sampling interval is 5.5 mm. The phase distribution of the electric field in three modes was experimentally measured.

Figure 8 shows the comparison of the plane phase diagrams of the three modes of the designed OAM antenna. From left to right(1, 0, and −1 modes), the first behavior is the field phase diagram simulated on HFSS. The second behavior is the plane field phase diagram of the microwave darkroom test,
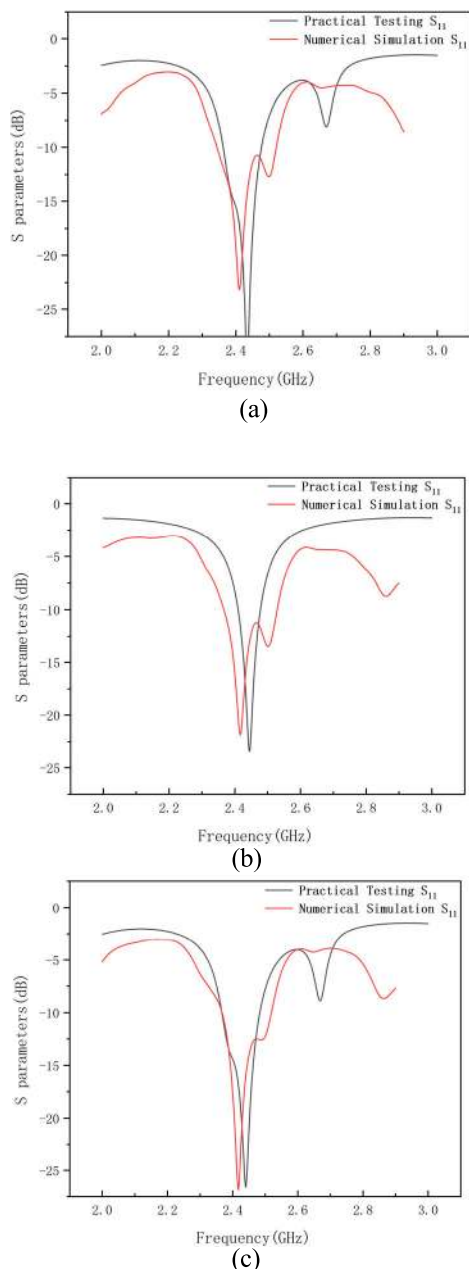
(a)

(b)

(c)

FIGURE 9. Numerical simulation and actual test values of OAM antenna S11 under different modes.

and the third behavior is the 3D phase diagram drawn from the measured data. From the comparison of the above simulation and the actual test, the designed antenna successfully generates the vortex electromagnetic wave. However, some problems are found between the simulation and test results. The spiral on the observation surface is rough. This problem is mainly because the sampling interval is excessively large. Unexpected parts are found in the phase diagram, which may be because of improper array radius setting and differences in chip bonding.

Figure 9 shows the comparison between the three modes of numerical simulation and actual test return loss parameters.

As shown in Figure 9 (b), the resonant frequency of the OAM antenna in the 0 mode agrees well with the numerical simulation. As shown in Figures 9 (a) and (c), the resonant frequency points are slightly offset when the OAM antenna is in the $+1$ and -1 modes, as previously discussed. The designed antenna has a return loss of less than -10 dB when generating three mode electromagnetic waves at 2.4 GHz. The antennas designed in different modes are less than -10 dB at 2.4GHz, the frequency of measured reflection coefficient $|S11| < -10$ dB ranges from 2.38 GHz to 2.55 GHz for the mode 0, and the frequency ranges from 2.35 GHz to 2.54 GHz for the mode ± 1.

V. CONCLUSION

In this paper, the numerical simulation and physical production test of the proposed integrated multimode OAM antenna based on RF switch are conducted. The test results show that the designed antenna can generate three modes $(+1, 0, -1)$ of vortex electromagnetic waves at 2.4 GHz, and the three modes can be dynamically switched by controlling the RF switch. The experimental results demonstrate the feasibility of RF switch application in the design of multimode vortex antenna. The designed antenna is of great significance in OAM multiplexing communication and high-resolution radar imaging.

REFERENCES

[1] Z. Guo, Y. Wang, Q. Zheng, C. Yin, Y. Yang, and Y. Gong, "Advances of research on antenna technology of vortex electromagnetic waves," *J. Radars*, vol. 8, no. 5, pp. 631–655, 2019.

[2] B. Thidé, H. Then, J. Sjöholm, K. Palmer, J. Bergman, T. D. Carozzi, Y. N. Istomin, N. H. Ibragimov, and R. Khamitova, "Utilization of photon orbital angular momentum in the low-frequency radio domain," *Phys. Rev. Lett.*, vol. 99, no. 8, p. 87701, Aug. 2007, doi: 10.1103/PhysRevLett.99.087701.

[3] J. C. García-Escartín and P. Chamorro-Posada, "Quantum multiplexing with the orbital angular momentum of light," *Phys. Rev. A, Gen. Phys.*, vol. 78, no. 6, p. 62320, Dec. 2008, doi: 10.1103/PhysRevA.78.062320.

[4] F. E. Mahmouli and S. Walker, "Orbital angular momentum generation in a 60 GHz wireless radio channel," in *Proc. 20th Telecommun. Forum (TELFOR)*, Nov. 2012, pp. 315–318.

[5] Q. Bai, A. Tennant, and B. Allen, "Experimental circular phased array for generating OAM radio beams," *Electron. Lett.*, vol. 50, no. 20, pp. 1414–1415, Sep. 2014, doi: 10.1049/el.2014.2860.

[6] L. Ma, C. Chen, L. Zhou, S. Jiang, and H. Zhang, "Single-layer transmissive metasurface for generating OAM vortex wave with homogeneous radiation based on the principle of Fabry–Pérot cavity," *Appl. Phys. Lett.*, vol. 114, no. 8, Feb. 2019, Art. no. 081603, doi: 10.1063/1.5081514.

[7] Y. Tan, L. Li, and H. Ruan, "Erratum for: An efficient approach to generate microwave vector vortex fields based on metasurface," *Microw. Opt. Technol. Lett.*, vol. 57, no. 9, p. 2228, Sep. 2015, doi: 10.1002/mop.29246.

[8] H. Li, L. Kang, F. Wei, Y.-M. Cai, and Y.-Z. Yin, "A low-profile dual-polarized microstrip antenna array for dual-mode OAM applications," *IEEE Antennas Wireless Propag. Lett.*, vol. 16, pp. 3022–3025, 2017, doi: 10.1109/LAWP.2017.2758520.

[9] B. Liu, Y. Cui, and R. Li, "A broadband dual-polarized Dual-OAM-mode antenna array for OAM communication," *IEEE Antennas Wireless Propag. Lett.*, vol. 16, pp. 744–747, 2017, doi: 10.1109/LAWP.2016.2601615.

[10] S. V. Hum and J. Perruisseau-Carrier, "Reconfigurable reflectarrays and array lenses for dynamic antenna beam control: A review," *IEEE Trans. Antennas Propag.*, vol. 62, no. 1, pp. 183–198, Jan. 2014, doi: 10.1109/TAP.2013.2287296.

[11] Y.-Y. Wang, Y.-X. Du, L. Qin, and B.-S. Li, "An electronically mode reconfigurable orbital angular momentum array antenna," *IEEE Access*, vol. 6, pp. 64603–64610, 2018, doi: 10.1109/ACCESS.2018.2877782.

[12] B. Liu, G. Lin, Y. Cui, and R. Li, "An orbital angular momentum (OAM) mode reconfigurable antenna for channel capacity improvement and digital data encoding," *Sci. Rep.*, vol. 7, no. 1, pp. 1–9, Dec. 2017, doi: 10.1038/s41598-017-10364-4.

[13] Q. Liu, Z. N. Chen, Y. Liu, F. Li, Y. Chen, and Z. Mo, "Circular polarization and mode reconfigurable wideband orbital angular momentum patch array antenna," *IEEE Trans. Antennas Propag.*, vol. 66, no. 4, pp. 1796–1804, Apr. 2018, doi: 10.1109/TAP.2018.2803757.

[14] Y.-M. Zhang and J.-L. Li, "An orbital angular momentum-based array for in-band full-duplex communications," *IEEE Antennas Wireless Propag. Lett.*, vol. 18, no. 3, pp. 417–421, Mar. 2019, doi: 10.1109/LAWP.2019.2893035.

[15] L. Kang, H. Li, J. Zhou, S. Zheng, and S. Gao, "A mode-reconfigurable orbital angular momentum antenna with simplified feeding scheme," *IEEE Trans. Antennas Propag.*, vol. 67, no. 7, pp. 4866–4871, Jul. 2019, doi: 10.1109/TAP.2019.2916595.

[16] S. M. Mohammadi, L. K. S. Daldorff, J. E. S. Bergman, R. L. Karlsson, B. Thide, K. Forozesh, T. D. Carozzi, and B. Isham, "Orbital angular momentum in radio—A system study," *IEEE Trans. Antennas Propag.*, vol. 58, no. 2, pp. 565–572, Feb. 2010, doi: 10.1109/TAP.2009.2037701.

[17] L. Allen, M. W. Beijersbergen, R. J. C. Spreeuw, and J. P. Woerdman, "Orbital angular momentum of light and the transformation of Laguerre–Gaussian laser modes," *Phys. Rev. A, Gen. Phys.*, vol. 45, no. 11, pp. 8185–8189, Jun. 1992, doi: 10.1103/PhysRevA.45.8185.

[18] Y. Gong, R. Wang, Y. Deng, B. Zhang, N. Wang, N. Li, and P. Wang, "Generation and transmission of OAM-carrying vortex beams using circular antenna array," *IEEE Trans. Antennas Propag.*, vol. 65, no. 6, pp. 2940–2949, Jun. 2017, doi: 10.1109/TAP.2017.2695526.

[19] A. E. Willner, H. Huang, Y. Yan, Y. Ren, N. Ahmed, G. Xie, C. Bao, L. Li, Y. Cao, Z. Zhao, J. Wang, M. P. J. Lavery, M. Tur, S. Ramachandran, A. F. Molisch, N. Ashrafi, and S. Ashrafi, "Optical communications using orbital angular momentum beams," *Adv. Opt. Photon.*, vol. 7, no. 1, pp. 66–106, Mar. 2015, doi: 10.1364/AOP.7.000066.

[20] J. Wu, Z. Zhang, X. Ren, Z. Huang, and X. Wu, "A broadband electronically mode-reconfigurable orbital angular momentum metasurface antenna," *IEEE Antennas Wireless Propag. Lett.*, vol. 18, no. 7, pp. 1482–1486, Jul. 2019, doi: 10.1109/LAWP.2019.2920695.

[21] X. Meng, J. Wu, Z. Wu, T. Qu, and L. Yang, "Dual-polarized reflectarray for generating dual beams with two different orbital angular momentum modes based on independent feeds in C-and X-bands," *Opt. Express*, vol. 26, no. 18, p. 23185, Sep. 2018, doi: 10.1364/OE.26.023185.
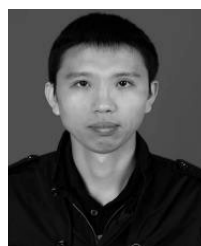
HUAN LIU received the B.S. degree in electronic information engineering from the Inner Mongolia University of Science and Technology, Baotou, China, in 2019, where he is currently pursuing the M.S. degree in information and communication engineering. His current research interests include OAM antennas and smart antenna technology.

LING QIN received the B.S. degree in communication engineering from the Chengdu University of Information Technology, Chengdu, China, in 2001, the M.S. degree in automation from the Xi'an University of Technology, Xi'an, China, in 2007, and the Ph.D. degree in automation from Chang'an University, Xi'an, in 2018.

She has served as a Lecturer and a Professor with the School of Information Engineering, Inner Mongolia University of Science and Technology, Baotou, from 2007 to 2012. She has published more than ten articles. Her research interest includes optical communication technique. She is currently a Reviewer with the National Natural Science Foundation of China, Chinese core journals *China Laser* and *Journal of Optics*, included by EI and a member of the organizing committee at the 2018 ISTCCA International Academic Conference. She has published more than 50 articles in important domestic and foreign journals and international academic conferences.

YONG-XING DU received the B.S. degree in communication engineering from the Chengdu University of Information Technology, Chengdu, China, in 2001, and the M.S. degree in electronic circuit and system and the Ph.D. degree in microelectronics and solid electronics from the Xi'an University of Technology, Xi'an, China, in 2007 and 2014, respectively.

He has served as a Research Assistant and a Lecturer with the School of Information Engineering, Inner Mongolia University of Science and Technology, Baotou, from 2001 to 2007 and 2007 to 2012, respectively, where he has been a Professor, since 2018. His main research interests include numerical calculation of electromagnetic fields, new microwave radiators, attenuation of black barrier effects, and beam synthesis. He is a Senior Member of the Chinese Institute of Electronics. He is also an Editor of the *American Journal of Traffic and Transportation Engineering* and the *Journal of Electronic Research and Application* and a Reviewer of IEEE Access, the IEEE MWCL, *Optical and Quantum Electronics*, the *International Journal of Electronics and Communications*, the Asia-Pacific Microwave Conference, *Measurement and Control Technology*, the *Journal of Optics*, *Laser* journal, and *Optical Communication Technology*.

BAO-SHAN LI received the B.S. degree in radio technology from Northeastern University, Shenyang, China, in 1986, and the M.S. degree in communication engineering from the Inner Mongolia University of Technology, Hohhot, China, in 2007.

He has served as a Lecturer and an Associate Professor with the School of Information Engineering, Inner Mongolia University of Science and Technology, Baotou, from 1986 to 1999 and 1999 to 2008, respectively, where he has been a Professor, since 2008. He has authored more than 30 articles. His current research interests include the application research of RFID and the IoT technology.

• • •